Hausdorff dimension and conformal dynamics III: Computation of dimension

Curtis T. McMullen*

3 October, 1997

Abstract

This paper presents an eigenvalue algorithm for accurately computing the Hausdorff dimension of limit sets of Kleinian groups and Julia sets of rational maps. The algorithm is applied to Schottky groups, quadratic polynomials and Blaschke products, yielding both numerical and theoretical results.

Dimension graphs are presented for

(a) the family of Fuchsian groups generated by reflections in 3 symmetric geodesics;
(b) the family of polynomials $f_c(z) = z^2 + c$, $c \in [-1, 1/2]$; and
(c) the family of rational maps $f_t(z) = z/t + 1/z$, $t \in (0, 1]$.

We also calculate $\mathrm{H.dim}(\Lambda) \approx 1.305688$ for the Apollonian gasket, and $\mathrm{H.dim}(J(f)) \approx 1.3934$ for Douady's rabbit, where $f(z) = z^2 + c$ satisfies $f^3(0) = 0$.

Contents

*Research partially supported by the NSF. 1991 Mathematics Subject Classification: Primary 58F23; Secondary 58F11, 30F40.

1 Introduction

Conformal dynamical systems such as Kleinian groups and rational maps are a rich source of compact sets in the sphere with fractional Hausdorff dimension. The limit sets and Julia sets of these dynamical systems have been much studied, although few concrete values for their dimensions have been determined.

In this paper we present an eigenvalue algorithm for accurately computing the Hausdorff dimension of limit sets and Julia sets in the case of expanding dynamics. We apply the algorithm to Schottky groups, quadratic polynomials and Blaschke products, obtaining both numerical and theoretical results.

In more detail, we consider the following examples.

1. *Schottky groups.* Our first examples (§3) are Kleinian groups generated by reflections in circles.

   Let Γ_θ be the Fuchsian group generated by reflections in three disjoint symmetric circles, each orthogonal to S^1 and meeting S^1 in an arc of length $0 < \theta \le 2\pi/3$. Since the limit set of this group is contained in S^1, we have $0 < \mathrm{H.\,dim}(\Lambda(\Gamma_\theta)) \le 1$. Using the eigenvalue algorithm, we graph the dimension of the limit set as θ varies. We also obtain results on the asymptotic behavior of the dimension:

   $$\mathrm{H.\,dim}(\Lambda(\Gamma_\theta)) \sim \frac{\log 2}{12 - 2\log\theta} \asymp \frac{1}{|\log\theta|}$$

   as $\theta \to 0$, while

   $$1 - \mathrm{H.\,dim}(\Lambda(\Gamma_\theta)) \asymp \sqrt{2\pi/3 - \theta}$$

   as $\theta \to 2\pi/3$.

2. *Hecke groups.* For the Fuchsian group Γ_r generated by reflections in the lines $\mathrm{Re}\, z = \pm 1$ and the circle $|z| = r$, $0 < r \le 1$, the limit set satisfies $1/2 < \mathrm{H.\,dim}(\Lambda(\Gamma_r)) \le 1$ because of the rank 1 cusp at $z = \infty$. We find

   $$\mathrm{H.\,dim}(\Lambda(\Gamma_r)) = \frac{1+r}{2} + O(r^2)$$

   as $r \to 0$, while

   $$1 - \mathrm{H.\,dim}(\Lambda(\Gamma_r)) \asymp \sqrt{1-r}$$

   as $r \to 1$. The group Γ_r is commensurable to the *Hecke group*

   $$H_R = \langle z \mapsto z + R, z \mapsto -1/z\rangle, \quad R = 2/r,$$

so the limit sets of Γ_r and H_R have the same dimension. Note that H_2 has index 3 in $SL_2(\mathbb{Z})$.

3. *The Apollonian gasket.* For a more complex example, consider the group Γ generated by reflections in 4 mutually tangent circles. Its limit set is the *Apollonian gasket.* The gasket can also be obtained by starting with 3 tangent circles, repeatedly packing new circles into the complementary interstices, and taking the closure. The eigenvalue algorithm yields the estimate

$$\mathrm{H.\,dim}(\Lambda(\Gamma)) \approx 1.305688,$$

compatible with the bounds $1.300 < \mathrm{H.\,dim}(\Lambda) < 1.315$ obtained by Boyd [5].

4. *Quadratic polynomials.* In §5 we consider the quadratic polynomials $f_c(z) = z^2 + c$. We present a graph of $\mathrm{H.\,dim}\, J(f_c)$ for $c \in [-1, 1/2]$, displaying Ruelle's formula

$$\mathrm{H.\,dim}(J(f_c)) \quad = \quad 1 + \frac{|c|^2}{4 \log 2} + O(|c|^3)$$

for c small, and exhibiting the discontinuity at $c = 1/4$ studied by Douady, Sentenac and Zinsmeister [9].

5. *Douady's rabbit.* For an example with $c \notin \mathbb{R}$, we take $c \approx -0.122561 + 0.744861i$ such that $f_c^3(0) = 0$. The Julia set of this map is known as *Douady's rabbit*, and we calculate

$$\mathrm{H.\,dim}\, J(f_c) \approx 1.3934.$$

6. *Blaschke products.* Any proper holomorphic map $f(z)$ of the unit disk to itself can be expressed as a *Blaschke product.* Like a Fuchsian group, the Julia set of such an f is contained in the unit circle.

   In §6 we conclude with two families of such mappings, reminiscent of the Fuchsian examples (1) and (2) above. For convenience we replace the unit disk with the upper half-plane.

   In the first family,
$$f_t(z) = \frac{z}{t} - \frac{1}{z},$$
$0 < t \leq 1$, the dynamics on the Julia set is highly expanding for t near 0, while $z = \infty$ becomes a parabolic fixed-point for f_t when $t = 1$. A

similar transition occurs in the family Γ_θ, when the generating circles become tangent at $\theta = 2\pi/3$. We present a graph of $\operatorname{H.dim}(J(f_t))$, and show

$$\operatorname{H.dim} J(f_t) \sim \frac{\log 2}{\log\left(\frac{2}{t} - 1\right)} \asymp \frac{1}{|\log t|}$$

as $t \to 0$, while $\operatorname{H.dim} J(f_t) \to 1$ as $t \to 1$.

The second family,

$$f_r(z) = z + 1 - \frac{r}{z},$$

$0 < r < \infty$, behaves like a combination of the two generators of the Hecke group H_R above. It has a parabolic point at $z = \infty$ for all r, and thus $1/2 < \operatorname{H.dim} J(f_r) < 1$. We find

$$\operatorname{H.dim} J(f_r) = \frac{1 + \sqrt{r}}{2} + O(r)$$

as $r \to 0$, while $\operatorname{H.dim} J(f_r) \to 1$ as $r \to \infty$.

Dimensions for these examples are tabulated in the Appendix.

Spectrum of the Laplacian. For the Fuchsian groups Γ considered in families (1) and (2) above, the least eigenvalue of the Laplacian on the hyperbolic surface is related to $D = \operatorname{H.dim} \Lambda(\Gamma)$ by

$$\lambda_0(\mathbb{H}^2/\Gamma) = D(1 - D)$$

(see [25], [17, Thm. 2.1]). Thus our dimension calculations also yield information on the bottom of the spectrum of the Laplacian. Similarly for the Apollonian 3-manifold of example (3) we obtain

$$\lambda_0(\mathbb{H}^3/\Gamma) = D(2 - D) \approx 0.399133.$$

Markov partitions. The eigenvalue algorithm we use to compute Hausdorff dimensions applies to general expanding conformal dynamical systems (§2). It requires a Markov partition $\mathcal{P} = \langle (P_i, f_i) \rangle$ such that $\bigcup P_i$ contains the support of the Hausdorff measure μ, and the conformal maps f_i generating the dynamics satisfy

$$\mu(f_i(P_i)) = \sum_{i \mapsto j} \mu(P_j).$$

(Here $i \mapsto j$ means $\mu(f_i(P_i) \cap P_j) > 0$.) From this combinatorial data the algorithm determines a transition matrix

$$T_{ij} = |f_i'(y_{ij})|^{-1}$$

with $y_{ij} \in P_i \cap f_i^{-1}(P_j)$. An estimate $\alpha(\mathcal{P})$ for the dimension of μ is then found by setting the spectral radius

$$\lambda(T^\alpha) = 1,$$

and solving for α. This estimate is improved by refining the partition; at most $O(N)$ refinements are required to obtain N digits of accuracy.

For a Schottky group, a Markov partition is given simply by the disjoint disks bounded by the generating circles.

For a polynomial $f(z)$ of degree d, a Markov partition $\mathcal{P} = \langle (P_i, f) \rangle$ can be defined using the boundary values

$$\phi : S^1 \to J(f_c)$$

of the Riemann mapping conjugating z^d to $f_c(z)$ on the basin of infinity. This ϕ exists whenever f is expanding and the Julia set is connected. Although ϕ is often many-to-one, we show in §4 that

$$\mu(\phi(I) \cap \phi(I')) = 0$$

for disjoint intervals $I, I' \subset S^1$ (except when f is a Chebyshev polynomial). Then the partition can be defined by $P_i = \phi(I_i)$, where $\langle I_i \rangle$ gives a Markov partition for $z \mapsto z^d$ on S^1.

Notes and references. The present paper evolved from the preprint [19] written in 1984; many of the results of that preprint appear in §2 and §3 below.

Bowen applied the machinery of symbolic dynamics, Markov partitions and Gibbs states to study the Hausdorff dimension of limit sets in [4]. Bodart and Zinsmeister studied $\operatorname{H.dim} J(z^2 + c)$ using a Monte-Carlo algorithm [3]. See also [28] and [23] for calculations for quadratic polynomials.

This paper belongs to a three-part series. Parts I and II study the continuity of Hausdorff dimension in families of Kleinian groups and rational maps [17], [18]. The bibliographies to parts I and II provide further references.

Notation. $A \asymp B$ means $A/C < B < CB$ for some implicit constant C; $A \sim B$ means $A/B \to 1$.

2 Markov partitions and the eigenvalue algorithm

In this section we define Markov partitions for conformal dynamical systems equipped with invariant densities. We then describe an algorithm for computing the dimension of the invariant density in the expanding case. For rational maps and Kleinian groups, this computation gives the Hausdorff dimension of the Julia set or the limit set.

Definitions. A *conformal dynamical system* $\mathcal{F}$ on $S^n = \mathbb{R}^n \cup \{\infty\}$ is a collection of conformal maps

$$f : U(f) \to S^n$$

where the domain $U(f)$ is an open set in S^n.

An *$\mathcal{F}$-invariant density of dimension* δ is a finite positive measure μ on S^n such that

$$\mu(f(E)) \quad = \quad \int_E |f'(x)|^\delta \, d\mu \tag{2.1}$$

whenever $f|E$ is injective, $E \subset U(f)$ is a Borel set and $f \in \mathcal{F}$. Here the derivative is measured in the spherical metric, given by $\sigma = 2|dx|/(1+|x|^2)$ on $\mathbb{R}^n$.

More formally, a density of dimension δ is a map from conformal metrics to measures such that

$$\frac{d\mu(\rho_1)}{d\mu(\rho_2)} \quad = \quad \left(\frac{\rho_1}{\rho_2}\right)^\delta .$$

We have implicitly identified μ with $\mu(\sigma)$; however (2.1) holds with respect to any conformal metric ρ, so long as we use the measure $\mu(\rho)$ and take derivatives in the ρ-metric.

A *Markov partition* for $(\mathcal{F}, \mu)$ is a nonempty collection $\mathcal{P} = \langle (P_i, f_i) \rangle$ of connected compact *blocks* $P_i \subset S^n$, and *maps* $f_i \in \mathcal{F}$ defined on P_i, such that:

1. $f_i(P_i) \supset \bigcup_{i \mapsto j} P_j$, where the relation $i \mapsto j$ means $\mu(f(P_i) \cap P_j) > 0$;
2. f_i is a homeomorphism on a neighborhood of $P_i \cap f_i^{-1}(P_j)$, when $i \mapsto j$;
3. $\mu(P_i) > 0$;
4. $\mu(P_i \cap P_j) = 0$ if $i \neq j$; and
5. $\mu(f(P_i)) = \mu(\bigcup_{i \mapsto j} P_j) = \sum_{i \mapsto j} \mu(P_j)$.

Our Markov partitions will always be *finite*.

A Markov partition is *expanding* if there is a smooth conformal metric ρ on S^n and a constant ξ such that

$$|f_i'(x)|_\rho > \xi > 1$$

whenever $x \in P_i$ and $f_i(x) \in P_j$ for some j.

The *refinement*

$$\mathcal{R}(\mathcal{P}) = \langle (R_{ij}, f_i) \ : \ i \mapsto j \rangle$$

is the new Markov partition defined by

$$R_{ij} = f_i^{-1}(P_j) \cap P_i.$$

In other words, each block is subdivided by the pullback of $\mathcal{P}$; the maps remain the same on the subdivided blocks.

Proposition 2.1 *If $\mathcal{P}$ is an expanding Markov partition, then the blocks of $\mathcal{R}^n(\mathcal{P})$ have diameter $O(\xi^{-n})$, $\xi > 1$.*

Proof. Since each block P_j of $\mathcal{P}$ is connected, any two points in P_j can be joined by a smooth path of uniformly bounded length L, contained in the range of f_i whenever $i \mapsto j$. Under f_i^{-1}, this path shrinks by ξ^{-1} in the ρ-metric, so points in R_{ij} are at most distance $\xi^{-1}L$ apart. Iterating, we find the ρ-diameter of the blocks of $\mathcal{R}^n(\mathcal{P})$ is at most $\xi^{-n}L$, and since the ρ metric and the spherical metric are comparable we are done. ∎

The eigenvalue algorithm. Next we give an algorithm for computing the dimension δ of the density μ. Suppose we are given a Markov partition $\mathcal{P} = \langle (P_i, f_i) \rangle$, and *sample points* $x_i \in P_i$. The algorithm computes a sequence of approximations $\alpha(\mathcal{R}^n(\mathcal{P}))$ to δ and proceeds as follows:

1. For each $i \mapsto j$, solve for $y_{ij} \in P_i$ such that $f_i(y_{ij}) = x_j$.

2. Compute the transition matrix
$$T_{ij} \quad = \quad \begin{cases} |f_i'(y_{ij})|^{-1} & \text{if } i \mapsto j, \\ 0 & \text{otherwise.} \end{cases}$$

3. Solve for $\alpha(\mathcal{P}) \geq 0$ such that the spectral radius satisfies
$$\lambda(T^\alpha) = 1.$$
Here $(T^\alpha)_{ij} = T_{ij}^\alpha$ denotes T with each entry raised to the power α.

4. Output $\alpha(\mathcal{P})$ as an approximation to δ.

5. Replace $\mathcal{P}$ with its refinement $\mathcal{R}(\mathcal{P})$, define new sample points $x_{ij} = y_{ij} \in R_{ij}$, and return to step (1).

We expect to have $\alpha(\mathcal{P}) \approx \delta$. In fact the transition law (2.1) implies $m_i = \mu(P_i)$ is an approximate eigenvector for T^δ_{ij} with eigenvalue $\lambda = 1$. That is,

$$\begin{aligned} m_i &= \mu(P_i) = \sum_{i\mapsto j} \mu(f_i^{-1}(P_j)) = \sum \int_{P_j} |(f_i^{-1})'(x)|^\delta \, d\mu \\ &\approx \sum |f_i'(y_{ij})|^{-\delta} \mu(P_j) = \sum_j T^\delta_{ij} m_j. \end{aligned}$$

This argument can be used to prove the algorithm converges in the expanding case.

Theorem 2.2 *Let $\mathcal{P}$ be an expanding Markov partition for a conformal dynamical system $\mathcal{F}$ with invariant density μ of dimension δ. Then*

$$\alpha(\mathcal{R}^n(\mathcal{P})) \to \delta$$

as $n \to \infty$. At most $O(N)$ refinements are required to compute δ to N digits of accuracy.

Proof. First suppose $\mathcal{P}$ is expanding in the spherical metric. Let $\mathcal{P} = \langle (P_i, f_i) \rangle$ and $P_{ij} = P_i \cap f_i^{-1}(P_j)$. Define S_{ij} and U_{ij} as the minimum and maximum of $|f_i'(x)|^{-1}$ over P_{ij} when $i \mapsto j$, and set $S_{ij} = U_{ij} = 0$ otherwise. Then by expansion we have

$$S_{ij} \le T_{ij} \le U_{ij} < \xi^{-1} < 1$$

for some constant ξ. In particular $\lambda(T^\alpha)$ is a strictly decreasing function of α, so there is a unique solution to $\lambda(T^\alpha) = 1$.

We claim

$$S^\delta m \le m \le U^\delta m$$

where $m_i = \mu(P_i)$. In fact

$$m_i = \mu(P_i) = \sum_{i\mapsto j} \int_{P_j} |(f_i^{-1})'(x)|^\delta \, d\mu \ge \sum_j S^\delta_{ij} \mu(P_j) = (S^\delta m)_i,$$

and similarly for U. Thus

$$\lambda(S^\delta_{ij}) \le 1 \le \lambda(U^\delta_{ij})$$

by the theory of non-negative matrices [12, Ch. XIII].

Since f is C^2, we also have

$$U_{ij}/S_{ij} = 1 + O(\max \operatorname{diam} P_i).$$

Choose $\beta = O(\max \operatorname{diam} P_i)$ such that $\xi^\beta S^\delta \geq U^\delta$. Then $T^{\delta-\beta} \geq S^\delta \xi^\beta \geq U^\delta$, so

$$\lambda(T^{\delta-\beta}) \geq \lambda(U^\delta) \geq 1.$$

Similarly $\lambda(T^{\delta+\beta}) \leq 1$. By continuity, the solution to $\lambda(T^\alpha) = 1$ lies between these two exponents, so

$$|\alpha(\mathcal{P}) - \delta| \leq 2\beta = O(\max \operatorname{diam} P_i).$$

By Proposition 2.1, the blocks of $\mathcal{R}^n(\mathcal{P})$ have diameter $O(\xi^{-n})$, and thus $|\alpha(\mathcal{R}^n(\mathcal{P})) - \delta| = O(\xi^{-n})$. In particular $O(N)$ refinements suffice to insure an error of less than 10^{-N}.

For the general case, in which we have expansion for a metric $\rho \neq \sigma$, note that the above argument works if we replace T by

$$\widetilde{T}_{ij} \;=\; |f_i'(y_{ij})|_\rho^{-1} \;=\; \frac{\rho(y_{ij})}{\sigma(y_{ij})} \frac{\sigma(x_j)}{\rho(x_j)} T_{ij}.$$

But for a fine partition, $y_{ij} \approx x_i$ and thus $\widetilde{T} \approx MTM^{-1}$ for the diagonal matrix with $M_{ii} = \rho(x_i)/\sigma(x_i)$. Since $\lambda(\widetilde{T}) = \lambda(MTM^{-1})$, we obtain exponential fast convergence to δ in the general case as well. ■

Practical considerations. To conclude this section we make some remarks on the practical implementation of the eigenvalue algorithm.

1. The algorithm only requires the combinatorics of the initial partition, the sample points x_i, and the ability to compute f_i^{-1} and f_i'. It does not keep track of the blocks of the partition $\mathcal{P}$.

2. In most applications the dynamics is eventually surjective, so the matrix T is *primitive* ($T^{\circ n} > 0$ for some power n). In this case the Perron-Frobenius theory shows the spectral radius $\lambda(T^\alpha)$ and its unique associated eigenvector can be found by iterating T^α on an arbitrary positive vector. Then $\lambda(T^\alpha) = 1$ can be solved by Newton's method.

3. As in the proof above, the same algorithm yields rigorous upper and lower bounds for the dimension δ by replacing T_{ij} with upper and lower bounds for $|f_i'|^{-1}$ on P_{ij}.

These bounds are sometimes quite conservative. The accuracy of the calculations presented below was estimated by observing the change in $\alpha(\mathcal{P})$ under refinement. These calculations should therefore be regarded as empirical results, at least to the full accuracy given.

4. In practice the algorithm is modified to adaptively refine only those blocks of the partition that exceed a critical diameter r. The reason is that best results are obtained if all the blocks are nearly the same size; otherwise, accurate calculations with small blocks are destroyed by the errors larger blocks introduce.

5. The number of nonzero entries per row of the transition matrix T remains constant as $\mathcal{P}$ is refined, so using sparse matrix methods T requires storage $O(|\mathcal{P}|)$ instead of $|\mathcal{P}|^2$.

6. In practice $\bigcup P_i \subset \mathbb{R}^n$ and we compute $|f_i'|$ in the Euclidean metric.

3 Schottky groups

In this section we consider Kleinian groups $\Gamma \subset \mathrm{Isom}(\mathbb{H}^3)$ generated by reflections.

Let S^2_∞ denote the boundary of hyperbolic 3-space $\mathbb{H}^3$ in the Poincaré ball model. The conformal automorphisms of S^2_∞ extend to give the full isometry group of $\mathbb{H}^3$. We identify S^2_∞ with the Riemann sphere $\widehat{\mathbb{C}} = \mathbb{C} \cup \{\infty\}$.

Every circle $C \subset S^2_\infty$ bounds a plane $H(C) \subset \mathbb{H}^3$; this plane is a Euclidean hemisphere normal to S^2_∞. The space of all circles forms a manifold, naturally identified with the Grassmannian $\mathcal{H}^3$ of planes in $\mathbb{H}^3$.

Consider a configuration $\mathcal{C} = \langle C_i \rangle$ of $d \geq 3$ circles in S^2_∞ bounding disks $D(C_i) \subset S^2_\infty$ with disjoint interiors. (The circles can be tangent but they cannot overlap or nest.) The space of all such configurations forms a closed set $\mathcal{S}_d \subset (\mathcal{H}^3)^d$.

Any circle $C \subset S^2_\infty$ determines a conformal reflection $\rho : S^2_\infty \to S^2_\infty$ fixing C, whose extension to $\mathbb{H}^3$ is a reflection through the plane $H(C)$. For $\mathcal{C} \in \mathcal{S}_d$ let $\Gamma(\mathcal{C})$ be the *Schottky group* generated by the reflections ρ_i through C_i, $i = 1, \ldots, d$.

The region outside the solid hemispheres bounded by $\langle H(C_i) \rangle$ gives a finite-sided fundamental domain for $\Gamma(\mathcal{C})$, and thus $\Gamma(\mathcal{C})$ is geometrically finite. The orientable double-cover of $M = \mathbb{H}^3/\Gamma(\mathcal{C})$ is a handlebody of genus $d - 1$. Any cusps of M are rank one and correspond bijectively to pairs of tangent circles in $\mathcal{C}$. Thus $\Gamma(\mathcal{C})$ is convex cocompact iff the circles in $\mathcal{C}$ are pairwise disjoint; equivalently, iff $\mathcal{C} \in \operatorname{int} \mathcal{S}_d$.

Theorem 3.1 *The function* $\mathrm{H.dim}\,\Lambda(\Gamma(\mathcal{C}))$ *is continuous on* $\mathcal{S}_d$ *and real-analytic on* $\operatorname{int} \mathcal{S}_d$.

Proof. Let $\mathcal{C}_n \to \mathcal{C}$ in $\mathcal{S}_d$. The generating reflections converge, so $\Gamma(\mathcal{C}_n) \to \Gamma(\mathcal{C})$ algebraically. By [17, Thm. 1.4], to prove continuity of the dimension of the limit set it suffices to prove all accidental parabolics converge radially. This means if $\gamma \in \Gamma(\mathcal{C})$ is the generator of a maximal parabolic subgroup, and $\gamma = \lim \gamma_n \in \Gamma(\mathcal{C}_n)$, then $\lambda_n \to 1$ radially, where λ_n is the derivative of γ_n at its attracting or parabolic fixed-point.

Now after conjugation in $\Gamma(\mathcal{C})$, we can assume $\gamma = \rho_i \rho_j$ is a product of reflections through a pair of tangent circles $C_i, C_j \in \mathcal{C}$. Thus $\gamma_n = \rho_{i,n}\rho_{j,n}$, the product of reflections through circles $C_{i,n}, C_{j,n} \in \mathcal{C}_n$. If these circles are disjoint, then γ_n acts on $\mathbb{H}^3$ by a pure translation along the common perpendicular to $H(C_{i,n})$ and $H(C_{j,n})$, and thus $\lambda_n \in \mathbb{R}$. Otherwise the circles are tangent and $\lambda_n = 1$. In either case $\lambda_n \to 1$ radially as was to be verified.

The real-analyticity of dimension on the space of convex cocompact groups is due to Ruelle [22]; see also [1]. ∎

To discuss a Markov partition for $\Gamma(\mathcal{C})$ we first need an invariant density.

Theorem 3.2 (Sullivan) *The limit set of a geometrically finite Kleinian group supports a unique nonatomic* Γ*-invariant density* μ *of total mass one. The dimension of the canonical density* μ *agrees with the Hausdorff dimension of the limit set.*

See [24], [17, Thm. 3.1].

Proposition 3.3 *Let* $\Gamma(\mathcal{C})$ *be convex cocompact. Then* $\mathcal{P} = \langle D(C_i), \rho_i \rangle$ *is an expanding Markov partition for* $\Gamma(\mathcal{C})$ *and its canonical density* μ.

Proof. Let $P_i = D(C_i)$, the closed disk in S^2_∞ bounded by C_i. By our description of the fundamental domain of $\Gamma(\mathcal{C})$ it is clear that the limit set Λ of $\Gamma(\mathcal{C})$ is contained in $\bigcup P_i$. By invariance, Λ is actually a Cantor covered by the successive refinements of $\mathcal{P}$. In particular Λ is disjoint from the generating circles C_i.

We now verify the axioms for a Markov partition.

(1) Since $\mu(C_i) = 0$, we have $i \mapsto j$ only if $i \neq j$; and since the circles in $\mathcal{C}$ are disjoint, we have

$$\rho_i(P_i) = S^2_\infty - \operatorname{int} P_i \supset \bigcup_{i \neq j} P_j.$$

(2) The map $\rho_i : S^2_\infty \to S^2_\infty$ is invertible, so it is a homeomorphism near P_i.

(3) Since $\Lambda \subset \bigcup P_i$, we have $\mu(P_i) > 0$ for some i, and hence $\mu(P_i) > 0$ for all i by (1).

(4,5) By assumption $P_i \cap P_j = \emptyset$ if $i \neq j$, and $\mu(f(P_i)) = \sum_{i \mapsto j} \mu(P_j)$ by (1) and the fact that $\Lambda \subset \bigcup P_i$.

Finally $\mathcal{P}$ is expanding because in the Euclidean metric, $|\rho_i'| > 1$ on $\operatorname{int} P_i$, and $\rho_i(P_j) \subset \operatorname{int} P_i$ is compact for each j. ∎

By Theorems 2.2 and 3.2 we have:

Corollary 3.4 *For disjoint circles,* $\mathrm{H.dim}\, \Lambda(\Gamma(\mathcal{C}))$ *can be computed by applying the eigenvalue algorithm to the Markov partition* $(D(C_i), \rho_i)$.

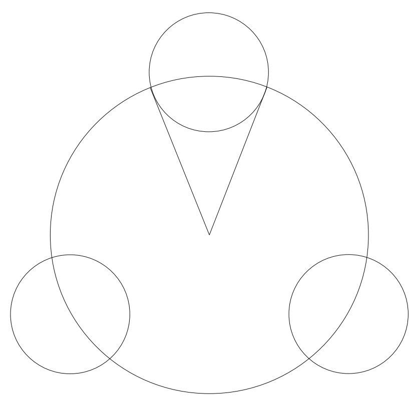

Figure 1. Generators for the Schottky group Γ_θ.

Example: Symmetric pairs of pants. For $0 < \theta < 2\pi/3$, let $\mathcal{C}_\theta$ be a symmetric configuration of 3 circles, each orthogonal to the unit circle $S^1 \subset \mathbb{C}$ and meeting S^1 in an arc of length θ (Figure 1). Let $\Gamma_\theta = \Gamma(\mathcal{C}_\theta)$.

Since the circles are orthogonal to S^1, we can consider Γ_θ as a group of isometries of $\mathbb{H}^2 \cong \Delta$ (the unit disk). The hyperbolic plane is tiled under this action by translates of a fundamental hexagon with sides alternating

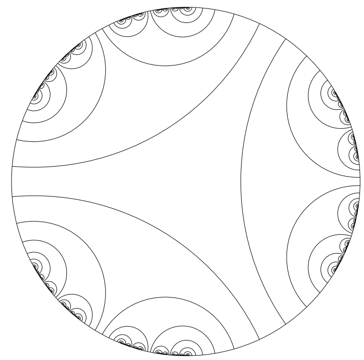

Figure 2. Tiling of $\mathbb{H}^2$ and Cantor set on S^1 of dimension ≈ 0.70055063.

along $\mathcal{C}_\theta$ and along S^1. The tiles accumulate on the limit set $\Lambda_\theta \subset S^1$, which is the full circle for $\theta = 2\pi/3$ and a Cantor set otherwise (Figure 2).

The orientable double cover X_θ of $\mathbb{H}^2/\Gamma_\theta$ is a pair of pants with $\mathbb{Z}/3$ symmetry. The surface $X_{2\pi/3}$ is the triply-punctured sphere, of finite volume; for $\theta < 2\pi/3$ the volume of X_θ is infinite.

Figure 3 displays the function $\mathrm{H.dim}(\Lambda_\theta)$, with θ measured in degrees. This graph was computed with the eigenvalue algorithm of §2, using the Markov partition coming from the disks bounded by the circles $\mathcal{C}_\theta$; the calculation is justified by Corollary 3.4.

The dotted line in the graph shows an asymptotic formula (3.1) for the dimension discussed below.

Theorem 3.5 *As $\theta \to 0$ we have*

$$\mathrm{H.dim}(\Lambda_\theta) \sim \frac{\log 2}{12 - 2\log\theta} \asymp \frac{1}{|\log\theta|}, \tag{3.1}$$

while for $\theta \to 2\pi/3$ we have

$$1 - \mathrm{H.dim}(\Lambda_\theta) \sim \lambda_0(X_\theta) \asymp \sqrt{2\pi/3 - \theta}. \tag{3.2}$$

Proof. Let $\mathcal{P} = \langle (P_i, \rho_i) \rangle$ with $P_i = D(C_i)$, $i = 1, 2, 3$. Then $\rho_1(P_1) \supset P_2 \sqcup P_3$, and similarly for the other blocks of $\mathcal{P}$.

For θ small the reflections ρ_i are nearly linear on $P_i \cap \rho_i(P_j)$, $i \neq j$, so $\alpha(\mathcal{P})$ already provides a good approximation to δ, by the proof of Theorem 2.2. To compute $\alpha(\mathcal{P})$, note the distance d between the centers of any pair

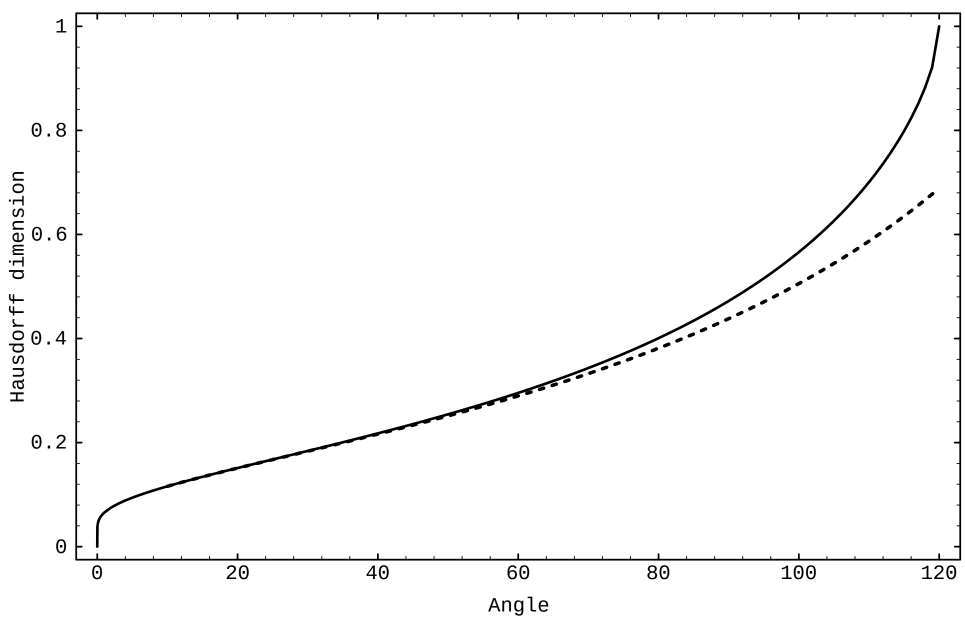

Figure 3. Dimension of the limit set of Γ_θ, and asymptotic formula.

of circles C_i and C_j is $\sqrt{3}$, and the radius of each circle is approximately $r = \theta/2$. Therefore

$$|\rho_i'| \sim \frac{r^2}{d^2} = \frac{\theta^2}{12}$$

inside P_j, $i \neq j$, and the transition matrix satisfies

$$T^\alpha_{ij} = \begin{pmatrix} 0 & t^\alpha & t^\alpha \\ t^\alpha & 0 & t^\alpha \\ t^\alpha & t^\alpha & 0 \end{pmatrix}$$

with $t \sim \theta^2/12$. The heighest eigenvalue of T^α is simply $2t^\alpha$; solving for $\lambda(T^\alpha) = 1$, we obtain (3.1).

To estimate $D_\theta = \mathrm{H.dim}\,\Lambda_\theta$ when the circles are almost tangent, we first note that $D_\theta \to 1$ as $\theta \to 2\pi/3$, by the continuity of D_θ (Theorem 3.1) and the fact that the limit set is S^1 when the circles touch. For $D_\theta > 1/2$ we have the relation $\lambda_0(X_\theta) = D_\theta(1 - D_\theta)$, where $\lambda_0(X_\theta)$ is the least eigenvalue of the L^2-Laplacian on the hyperbolic surface X_θ [25], [17, Thm. 2.1], which shows

$$1 - D_\theta \sim \lambda_0(X_\theta)$$

as $\theta \to 2\pi/3$.

Now for θ near $2\pi/3$, the convex core of X_θ is bounded by three short simple geodesics of equal length L_θ. These short geodesics control the least eigenvalue of the Laplacian; more precisely,

$$\lambda_0(X_\theta) \;=\; \inf \frac{\int_{X_\theta} |\nabla f|^2}{\int_{X_\theta} |f|^2} \asymp L_\theta,$$

because the quotient above is approximately minimized by a function with $f = 1$ in the convex core of X_θ, $f = 0$ in the infinite volume ends, and ∇f supported in standard collar neighborhoods of the short geodesics [7, Thm 1.1′]. A calculation with cross-ratios shows, for $C_1, C_2 \in \mathcal{C}_\theta$,

$$L_\theta = 2 d_{\mathbb{H}^2}(C_1, C_2) \asymp \sqrt{2\pi/3 - \theta},$$

and we obtain (3.2). ∎

Example: Hecke groups. As a second 1-parameter family, for $0 < r \leq 1$ let $\mathcal{C}_r = \langle C_1, C_2, C_3 \rangle$ consist of the circle $|z| = r$ and the lines $\operatorname{Re} z = \pm 1$ (union $z = \infty$). Let Λ_r be the limit set of $\Gamma_r = \Gamma(\mathcal{C}_r)$.

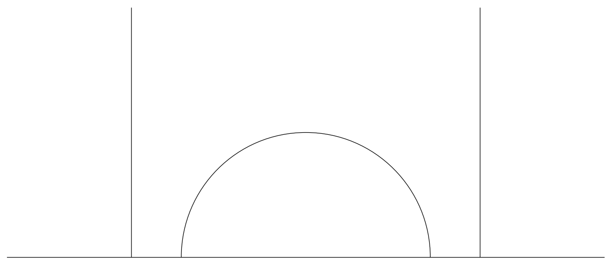

Figure 4. Fundamental domain for Γ_r in $\mathbb{H}$.

In this case Γ_r preserves the upper half-plane $\mathbb{H}$, and the orientable double-cover X_r of $\mathbb{H}/\Gamma_r$ is a pair of pants with one cusp and two infinite-volume ends. The cusp corresponds to $z = \infty$ in the fundamental domain for Γ_r (Figure 4).

The group Γ_r is closely related to the *Hecke group*

$$H_R = \left\langle z \mapsto -\frac{1}{z},\, z \mapsto z + R \right\rangle,$$

and the group

$$G_R = \left\langle z \mapsto \frac{z}{2Rz+1},\, z \mapsto z + 1 \right\rangle$$

studied in [17, §8], where $R = 2/r$. All three groups are commensurable; more precisely, there is a single hyperbolic surface Y_r that finitely covers $\mathbb{H}/\Gamma_r$, $\mathbb{H}/G_R$ and $\mathbb{H}/H_R$. Thus the limit sets of all three groups have the same dimension.

Theorem 3.6 *As $r \to 0$ we have*

$$\mathrm{H.dim}(\Lambda_r) = \frac{1+r}{2} + O(r^2), \tag{3.3}$$

while for $r \to 1$ we have

$$1 - \mathrm{H.dim}(\Lambda_r) \sim \lambda_0(X_r) \asymp \sqrt{1-r}. \tag{3.4}$$

Proof. For r small the limit set Λ_r is a Cantor set, consisting of $\{\infty\}$ union isometric pieces $\Lambda_r(n)$ concentrated near $z = 2n$, $n \in \mathbb{Z}$. We have

$$\Lambda_r(0) \quad = \quad \{0\} \cup \rho\left(\bigcup_{n \neq 0} \Lambda_r(n)\right),$$

where $\rho \in \Gamma_r$ denotes reflection through the circle of radius r. Letting μ denote the canonical measure for Γ_r in the Euclidean metric, we find

$$\mu(\Lambda_r(0)) = \sum_{n\neq 0} \int_{\Lambda_r(n)} |\rho'(x)|^\delta \, d\mu = 2\sum_{n>0} \left(\frac{r}{2n}(1+O(r))\right)^{2\delta} \mu(\Lambda_r(n)).$$

But $\mu(\Lambda_r(n)) = \mu(\Lambda_r(0))$, so we obtain

$$2\zeta(2\delta) = (r/2)^{-2\delta}(1+O(r)),$$

where ζ is the Riemann zeta-function. From this equation we find $\mathrm{H.\dim}(\Lambda_r) \to 1/2$, and then the more precise estimate (3.3) follows from the expansion

$$\zeta(s) = \frac{1}{s-1} + O(1)$$

near $s = 1$.

Equation (3.4) is proved by the same spectral argument as (3.2). ■

The proof of (3.3) just given is essentially an application of the eigenvalue algorithm to an infinite Markov partition.

Example: The Apollonian gasket. The well-known *Apollonian gasket* Λ is the limit set of $\Gamma(\mathcal{C})$ for a configuration of 4 mutually tangent circles. The gasket can also be constructed by starting with 3 tangent circles, repeatedly packing new circles into the complementary triangular interstices, and taking the closure (Figure 5).

The eigenvalue algorithm also serves to compute $\mathrm{H.\dim}\,\Lambda \approx 1.305688$. A sample adaptively refined Markov partition is shown in Figure 5; note that the blocks vary widely in size, due to the slow expansion near points of tangency.

Since $\Gamma(\mathcal{C})$ is geometrically finite but not convex cocompact, some additional remarks are needed to justify the algorithm in this case. For concreteness we assume the sample points x_i are chosen in the center of each circle C_i. The argument is based on continuity of $\mathrm{H.\dim}\,\Gamma(\mathcal{C})$ and the fact that the circles become disjoint under a computationally imperceptible perturbation. In more detail, one observes that the normalized eigenvector m_i for T_{ij} converges, under refinement of the Markov partition, to an invariant density μ for $\Gamma(\mathcal{C})$ of dimension $\delta = \lim \alpha(\mathcal{R}^n(\mathcal{P}))$. By analyzing the behavior near parabolic points, one finds (as in the proof of continuity of dimension, [17, Thm. 1.4]) that μ has no atoms. Thus μ is the canonical density and $\delta = \mathrm{H.\dim}\,\Lambda$, by Theorem 3.2.

Notes.

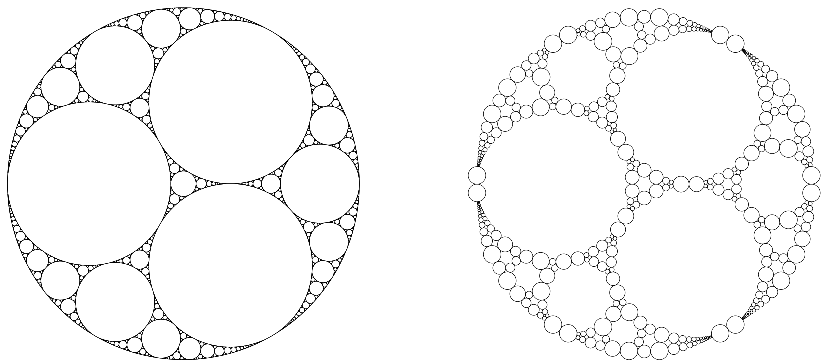

Figure 5. The Apollonian gasket, dimension ≈ 1.305688, and its Markov partition.

1. Doyle has shown there is a constant δ_0, independent of the number of circles, such that
$$\mathrm{H.}\dim \Lambda(\Gamma(\mathcal{C})) \leq \delta_0 < 2$$
for all configurations of circles bounding disjoint disks [10]. A similar result was proved earlier for reflections through disjoint spheres in S^n_∞, $n \geq 3$, by Phillips and Sarnak [21]. These authors also made numerical estimates for the dimension of the limit set of Schottky groups acting on S^2 by counting orbits.

   We originally developed the eigenvalue algorithm to investigate of the value of δ_0 for $\mathbb{H}^3$ [19].

2. Boyd has rigorously shown that $1.300197 < \mathrm{H.}\dim(\Lambda) < 1.314534$ for the Apollonian gasket [5], [11, §8.4].

3. The dimension estimate for Hecke groups can be generalized to higher dimensions as follows. Let Γ_r be generated by a lattice of translations L acting on $\mathbb{R}^n$, together with an inversion in the sphere of radius r. Then for $r \to 0$, we find
$$\mathrm{H.}\dim \Lambda_r = \frac{n}{2}\left(1 + \frac{\mathrm{vol}(B(r))}{\mathrm{vol}(\mathbb{R}^n/L)}\right) + O(r^{n+1}).$$
The proof uses the zeta function $\sum_{L\setminus 0} |\ell|^{-s}$.

The special case $L = \mathbb{Z}[i]$ (the Gaussian integers), $r = 1/2$, has been studied by Gardner and Mauldin in connection with complex continued fractions [13]. They prove the limit set satisfies $1 < \mathrm{H.dim}(\Lambda) < 2$. These bounds also follows from the general theory of geometrically finite groups with cusps [17, Cors. 2.2, 3.2].

4. A result similar to (3.3) for the Hecke groups appears in [2, Thm. 3].

4 Markov partitions for polynomials

In this section we construct, via external angles, a Markov partition for expanding polynomials.

The radial Julia set. A point $z \in \widehat{\mathbb{C}}$ belongs to the *radial Julia set* $J_{\mathrm{rad}}(f)$ if there exists an $r > 0$ so for all $\epsilon > 0$, there is an $n > 0$ and a neighborhood U of x with $\mathrm{diam}(U) < \epsilon$ such that

$$f^n : U \to B(f^n(x), r)$$

is a homeomorphism to a ball of spherical radius r. In other words, $z \in J_{\mathrm{rad}}(f)$ iff arbitrarily small neighborhoods of z can be blown up univalently to balls of definite size. Compare [18, §2].

Geometric finiteness. A rational map is *expanding* if its Julia set contains no critical points or parabolic points. More generally, if every critical point in $J(f)$ is preperiodic, then f is *geometrically finite.* From [18, Thm. 1.2] we have:

Theorem 4.1 *The Julia set of a geometrically finite map f carries a unique invariant density μ of dimension $\delta = \mathrm{H.dim}\, J(f)$ and total mass one. The canonical density μ is nonatomic and supported on the radial Julia set.*

External angles. For a polynomial $f(z)$, the *filled Julia set* $K(f)$ is defined as the set of $z \in \mathbb{C}$ such that $f^n(z)$ does not converge to infinity. When $J(f)$ is connected, there is a Riemann mapping

$$\Phi : (\mathbb{C} - \overline{\Delta}) \to (\mathbb{C} - K(f))$$

from the complement of the unit disk to the complement of the filled Julia set. Composing with a rotation, we can arrange that

$$\Phi(z^d) = f(\Phi(z)), \tag{4.1}$$

and this normalization is unique up to replacing $\Phi(z)$ with $\Phi(\alpha z)$ where $\alpha^{d-1} = 1$.

When f is geometrically finite, $J(f)$ is locally connected and Φ extends to a continuous map

$$\phi : S^1 \to J(f)$$

also obeying (4.1) [8, Exposé X] (see also [20, §17], [27]). The point $\phi(z) \in J(f)$ is said to have *external angle* z; a given point may have many external angles.

In this section we will show:

Theorem 4.2 (Polynomial partition) *Let $f(z)$ be an expanding polynomial with connected Julia set. Then $\mathcal{P} = (\phi(I_i), f)$ gives an expanding Markov partition for (f, μ), where*

$$I_i = \left[\frac{i-1}{d}, \frac{i}{d}\right]$$

under the identification $S^1 = \mathbb{R}/\mathbb{Z}$, and μ is the canonical density for f.

Corollary 4.3 *The eigenvalue algorithm applied to $\mathcal{P}$ computes* $\mathrm{H.dim}\, J(f)$.

Chebyshev polynomials. The *Chebyshev polynomial* $T_d(z)$ is defined by $T_d(\cos\theta) = \cos d\theta$; for example, $T_2(z) = 2z^2 - 1$. The map $T_d(z)$ is semiconjugate to $z \mapsto z^d$ under $\pi(z) = (z + z^{-1})/2$; that is,

$$T_d(\pi(z)) = \pi(z^d).$$

Thus the Julia set of T_d is $\pi(S^1) = [-1, 1]$.

To show $\mathcal{P}$ is a Markov partition, the main point is checking $\mu(P_i \cap P_j) = 0$. This point is handled by:

Theorem 4.4 (Essentially disjoint) *Let $f(z)$ be a geometrically finite polynomial with connected Julia set and canonical density μ. Then either:*

(a) $\mu(\phi(I) \cap \phi(J)) = 0$ for all disjoint intervals $I, J \subset S^1$; or

(b) $f(z)$ is conformally conjugate to the Chebyshev polynomial $T_d(z)$.

Proof. For any open interval $I \subset S^1$ let

$$D(I) = \frac{\mu(\phi(I) \cap \phi(S^1 - I))}{\mu(\phi(I))}$$

denote the density of points in $\phi(I)$ with external angles outside of I. Clearly $0 \leq D(I) \leq 1$. If $D(I) = 0$ for all I then $\mu(\phi(I) \cap \phi(J)) = 0$ for all pairs of disjoint intervals, which is case (a) of the Theorem.

Now suppose $D(I) > 0$ for some I. We will produce from I an interval with $D(I_\infty) = 1$.

Define $E \subset F$ by

$$\begin{aligned} E &= \phi(I) \cap \phi(S^1 - I), \\ F &= \phi(I); \end{aligned}$$

then $\mu(E) > 0$. By basic results in measure theory, [15, Cor. 2.14], almost every $x \in E \subset F$ is a point of density; that is,

$$\lim_{r \to 0} \frac{\mu(E \cap B(x,r))}{\mu(F \cap B(x,r))} = 1. \tag{4.2}$$

And since f is geometrically finite, almost every $x \in E$ belongs to the radial Julia set. This means there are infinitely many $n > 0$ and radii $r_n \to 0$ such that

$$f^n : B(x, r_n) \to U_n$$

is univalent with bounded distortion, and $B(f^n(x), r_0) \subset U_n$ [18, Thm. 1.2]. In other words $B(x, r_n)$ can be expanded by the dynamics to a region of definite size.

Choosing x satisfying both (4.2) and the radial expansion property above, and define $E_n \subset F_n \subset U_n$ by

$$\begin{aligned} E_n &= f^n(E \cap B(x, r_n)), \\ F_n &= f^n(F \cap B(x, r_n)). \end{aligned}$$

Since μ transforms by $|(f^n)'(z)|^\delta$, where $\delta = \mathrm{H.dim}(J(f))$, the Koebe distortion theorem and (4.2) imply

$$\mu(E_n)/\mu(F_n) \to 1.$$

Consider a maximal path $\phi(J_n) \subset \phi(I) \cap B(x, r_n)$ passing through x. That is, let J_n be a component of $I \cap \phi^{-1}(B(x, r_n))$ with $x \in \phi(J_n)$. Then for n large, this path begins and ends in $\partial B(x, r_n)$, so $\operatorname{diam} \phi(J_n) \asymp r$. Let $I_n = p^n(J_n)$ where $p(z) = z^d$; then

$$\operatorname{diam} \phi(I_n) \asymp r_0 \tag{4.3}$$

since $\phi(I_n) = f^n(\phi(J_n))$ begins and ends in ∂U_n.

We claim $D(I_n) \to 1$. To see this, note that injectivity of $f^n|B(x, r_n)$ implies injectivity of $p^n|\phi^{-1}(B(x, r_n))$. Thus every point in $\phi(I_n) \cap E_n$ has an external angle outside I_n, and we conclude that

$$D(I_n) \geq \frac{\mu(\phi(I_n) \cap E_n)}{\mu(\phi(I_n))}.$$

But $\phi(I_n) \subset F_n$, and from (4.3) we have $\mu(\phi(I_n)) > \epsilon > 0$ for all n. Since $\mu(E_n)/\mu(F_n) \to 1$, we find $D(I_n) \to 1$ as well.

Since μ has no atoms, $D(I_n)$ is a continuous function of the endpoints of I_n. Passing to a subsequence, we can assume I_n converges to an interval I_∞, nonempty by (4.3) . Then $D(I_\infty) = 1$.

Next we claim $\phi|I_\infty$ is injective. In fact, if the endpoints of $[a, b] \subset I_\infty$ are identified by ϕ, then $U = \phi((a, b))$ is disconnected from the rest of $J(f)$ by $\phi(a)$, and hence the external angles of U all lie in (a, b). Since $D(I_\infty) = 1$ we conclude $\mu(U) = 0$ which is only possible if $a = b$.

Now we show $f(z)$ is conjugate to $T_d(z)$. Since $\phi|I_\infty$ is injective and $p^n(I_\infty) = S^1$ for some n, we see $\phi = f^n \circ \phi \circ p^{-n}$ is locally injective outside a finite subset of S^1 (corresponding to critical values of f^n). Thus $J(f)$ is homeomorphic to a finite graph. Any vertex of $J(f)$ of degree 3 or more would give rise to vertices of degree at least 3 along an entire inverse orbit, so there are no such vertices and $J(f)$ is homeomorphic to a circle or an interval. In the circle case ϕ is a homeomorphism, contrary to our assumption that $D(I) > 0$.

Thus $J(f)$ is an interval with a pair of endpoints $E \subset \mathbb{C}$. After an affine conjugacy we can assume $E = \{-1, 1\}$. Let $\pi : \mathbb{C}^* \to \mathbb{C}$ be the degree two covering, branched over E, given by $\pi(z) = (z + z^{-1})/2$. By total invariance of $J(f)$, $f^{-1}(E) - E$ consists entirely of critical points of order 2. Thus f lifts to a rational map $g : \mathbb{C}^* \to \mathbb{C}^*$ satisfying $f(\pi(z)) = \pi(g(z))$. Any degree d rational map sending $\mathbb{C}^*$ to itself has the form $g(z) = \alpha z^{\pm d}$, and it follows easily that f is conjugate to the Chebyshev polynomial $T_d(z)$. ■

Proof of Theorem 4.2 (Polynomial partition). We verify the axioms for a Markov partition in §2.

(1) Letting $P_i = \phi(I_i)$, the semiconjugacy $\phi(z^d) = f(\phi(z))$ implies $f(P_i) = \bigcup P_i = J(f)$.

(2) By expansion, f is a local homeomorphism near $J(f)$. We have $P_{ij} = P_i \cap f^{-1}(P_j) = \phi(I_{ij})$ for an arc $I_{ij} \subset S^1$ of length $2\pi/d^2$; since z^d is injective on I_{ij}, f is a homeomorphism on a neighborhood of P_{ij}.

(3,4,5) Clearly $\mu(P_i) > 0$ by (1), and $\mu(P_i \cap P_j) = 0$ for $i \neq j$ by Theorem 4.4; thus $\mu(f(P_i)) = \mu(J(f)) = \sum_j \mu(P_j)$.

Finally expansion of f implies there is a conformal metric such with $|f'|_\rho > 1$ on $J(f)$ [16, Thm 3.13], so $\mathcal{P}$ is an expanding Markov partition. ■

Corollary 4.3 follows by Theorem 2.2.

5 Quadratic polynomials

In this section we discuss the dimension of the Julia set for the family of quadratic polynomials

$$f_c(z) = z^2 + c.$$

The forward orbit $f_c^n(0)$ of the critical orbit $z = 0$ converges to an attracting or superattracting cycle in $\mathbb{C}$ iff

(a) the Julia set $J(f_c)$ is connected, and
(b) f_c is expanding.

See [6, Ch. VIII], [16, Thm 3.13]. When these two conditions are satisfied, Theorem 4.2 furnishes a 2-block expanding Markov partition $\mathcal{P} = \langle (P_i, f_c) \rangle$ with $P_1 = \phi_c([0, 1/2])$ and $P_2 = \phi_c([1/2, 1])$, where

$$\phi_c : S^1 \cong \mathbb{R}/\mathbb{Z} \to J(f_c)$$

satisfies $\phi_c(2x) = f_c(\phi_c(z))$. Thus the dimension of the Julia set can be computed by the eigenvalue algorithm, according to Corollary 4.3.

For sample points, we take

$$\{x_1, x_2\} \quad = \quad \{\phi_c(1/4), \phi_c(3/4)\} \quad = \quad f_c^{-1}(-\beta_c),$$

where $\beta_c = \phi_c(0)$ is the 'β-fixed point' of f_c. Then $f^2(x_i) = \beta_c$, and the sample points for all refinements of $\mathcal{P}$ are also contained in the inverse orbit of β_c.

The same algorithm also serves to compute $\mathrm{H.\,dim}\, J(f_c)$ when the Julia set is a Cantor set. In this case an expanding Markov partition can be constructed using equipotentials in the basin of infinity.

Example: $\boldsymbol{z^2 - 1}$. For $c = -1$ the critical point of f_c is periodic of order 2; its Julia set, with $\mathrm{H.\,dim}(J(f_c)) \approx 1.26835$, is rendered in Figure 6.

Example: Douady's rabbit. For $c \approx -0.122561 + 0.744861i$, the critical point of f_c has period 3. Its Julia set, rendered in Figure 7, satisfies $\mathrm{H.\,dim}(J(f_c)) \approx 1.3934$.

Example: the real quadratic family. For $c \in \mathbb{R}$, $J(f_c)$ is connected iff $c \in [-2, 1/4]$. Outside this interval $J(f_c)$ is a Cantor set, and f_c is expanding.

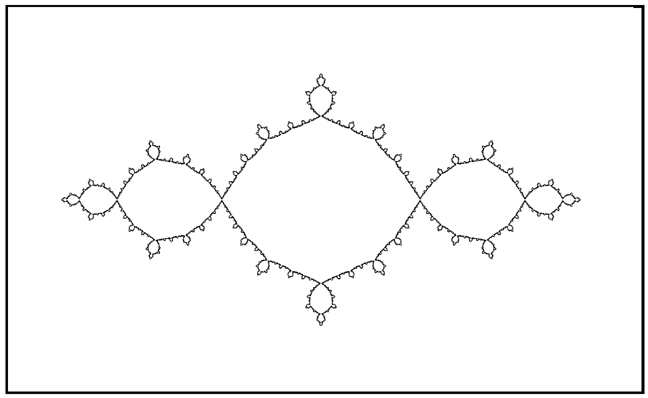

Figure 6. The Julia set for $z^2 - 1$, of dimension ≈ 1.26835.

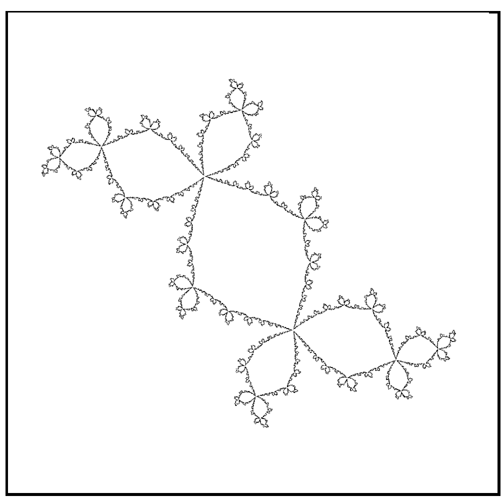

Figure 7. Douady's rabbit: dimension ≈ 1.3934.

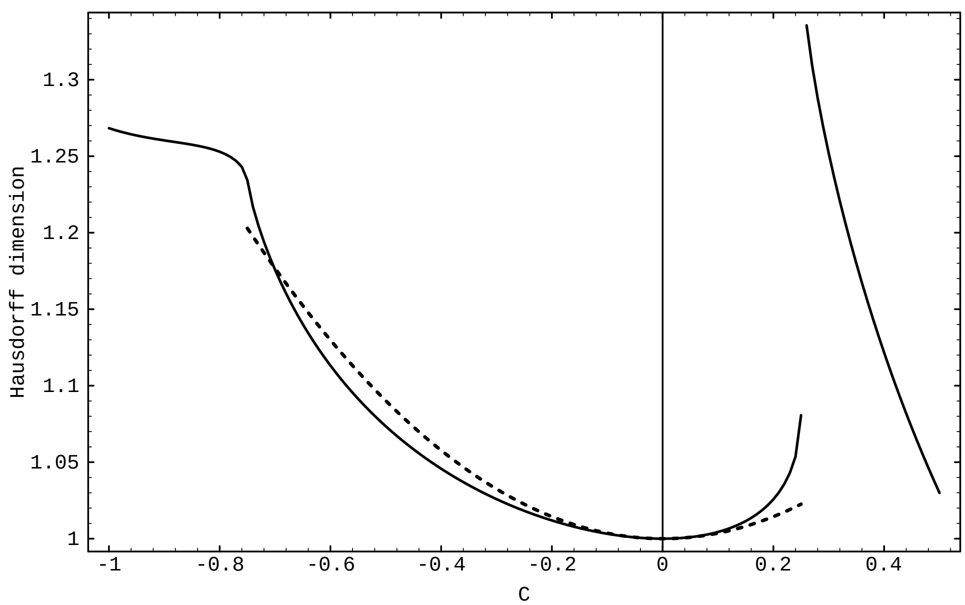

Figure 8. Dimension of quadratic Julia sets and Ruelle's formula.

The point $c = 1/4$ is parabolic; that is, f_c has a parabolic cycle ($z = 1/2$), so it is geometrically finite but not expanding.

As c decreases from $1/4$ along the real axis, the map f_c undergoes a sequence of period-doubling bifurcations at parabolic points c_n converging to the *Feigenbaum point* $c_{\mathrm{Feig}} \approx -1.401155$. The map f_c is expanding for all $c \in (c_{\mathrm{Feig}}, 1/4]$ outside this sequence c_n. In [18] we show:

Theorem 5.1 *The function* $\mathrm{H.dim}\, J(f_c)$ *is continuous on the interval* $(c_{Feig}, 1/4]$.

The graph of $\dim J(f_c)$ for $c \in [-1, 1/2]$, as determined by the eigenvalue algorithm, is plotted in Figure 8. One striking feature is the discontinuity at the parabolic point $c = 1/4$, studied in detail by Douady, Sentenac and Zinsmeister [9]. This discontinuity is due to the 'parabolic implosion' that results for $c = 1/4 + \epsilon$. The Julia sets for $c = 0.25$ and $c = 0.26$ are compared in Figure 9. As c increases past $1/4$, the parabolic point at $z = 1/2$ bifurcates into a pair of repelling fixed-points, off the real axis. The Julia set disintegrates discontinuously into a Cantor set as previously bounded orbits escape to infinity. It is likely at $\mathrm{H.dim}\, J(f_c)$ oscillates as $c \to 1/4$ from above; see [9].

The map f_c is expanding for $c \in (-3/4, 1/4)$. Ruelle showed $\mathrm{H.dim}\, J(f_c)$ is real-analytic at any point c where f_c is expanding, and computed the formula

$$\mathrm{H.dim}(J(f_c)) \;=\; 1 + \frac{|c|^2}{4 \log 2} + O(|c|^3)$$

for c near 0 [22]. This quadratic approximation is plotted as a dotted line in Figure 8.

A second parabolic bifurcation occurs as c decreases past $-3/4$, but $\mathrm{H.dim}\, J(f_c)$ is continuous there. In this case the parabolic fixed-point gives rise to an attracting cycle of order two, instead of a pair of repelling points. It seems likely that the dimension fails to be real-analytic at $c = -3/4$ or any other parabolic bifurcation.

Notes.

1. The results of a Monte-Carlo algorithm for computing $\mathrm{H.dim}\, J(f_c)$ are presented in [3].

2. A treatment of the relationship between the thermodynamic formalism and conformal dynamics, leading up to Ruelle's formula, is given in [29].

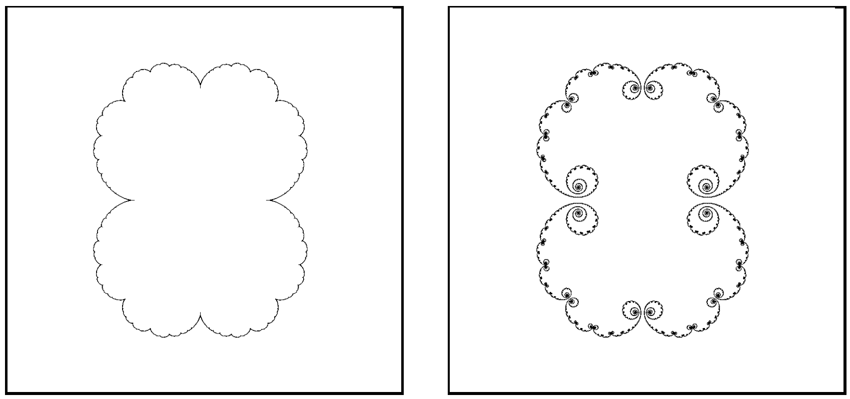

Figure 9. Parabolic implosion.

3. Ruelle's formula is extended in [28], which also includes some numerical calculations.

6 Quadratic Blaschke products

Let $f : \widehat{\mathbb{C}} \to \widehat{\mathbb{C}}$ be a degree d rational map that leaves invariant a round disk $D \subset \widehat{\mathbb{C}}$ (meaning $f^{-1}(D) = D$). Then up to conjugacy we can assume D is the unit disk, in which case f can be expressed as a *Blaschke product*

$$f(z) = e^{it} \prod_1^d \left(\frac{z - a_i}{1 - \overline{a_i} z} \right), \quad |a_i| < 1.$$

A Blaschke product behaves in many ways like a finitely-generated Fuchsian group; for example, its Julia set is contained in the unit circle, and f is always geometrically finite.

In this section we consider two 1-parameter families of quadratic Blaschke products that are reminiscent of the Schottky groups studied in §3. To make the formulas more convenient, we will normalize so the invariant disk D is the upper half-plane instead of the unit disk. Then we have $J(f) \subset \widehat{\mathbb{R}} = \mathbb{R} \cup \{\infty\}$.

Example I. For $0 < t \leq 1$ let

$$f_t(z) = \frac{z}{t} - \frac{1}{z} \cdot$$

By [18, Thm 1.4], $\mathrm{H.dim}\, J(f_t)$ is continuous for $t \in (0, 1]$ (and real-analytic on $(0, 1)$ by [22]).

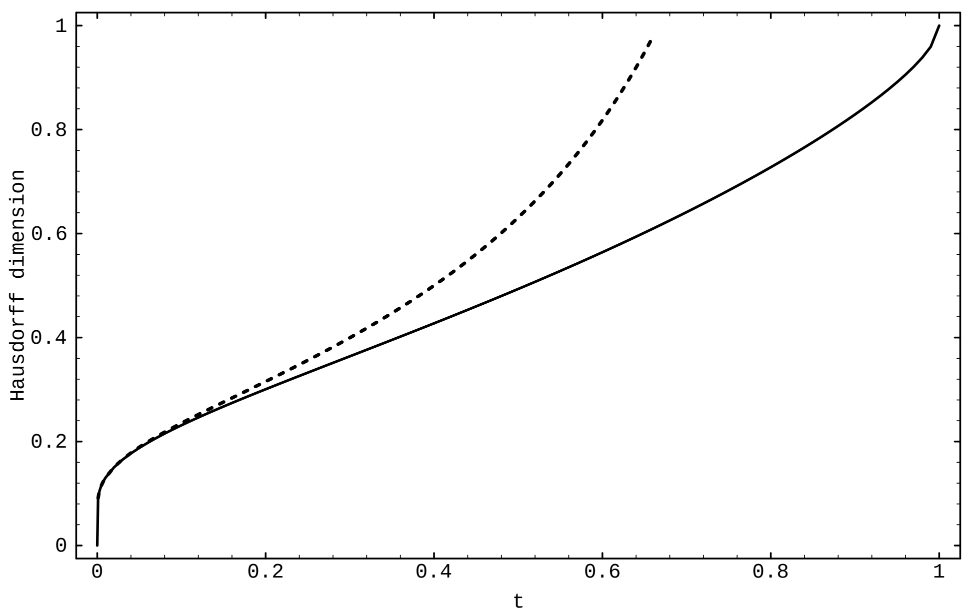

Figure 10. Dimension of the Julia set of $f_t(z) = z/t - 1/z$, and asymptotic formula.

The Julia set of $f_1(z) = z - 1/z$ is $\widehat{\mathbb{R}}$. Indeed, $z = \infty$ is a parabolic point with two petals, repelling along the real directions at $z = \infty$. Since any point in the Fatou set of f_1 must lie in the basin of $z = \infty$, no such point can be real.

For $t < 1$, $z = \infty$ is an attracting fixed-point of f_t with multiplier t, both critical points converge to ∞ and f_t is expanding. The Julia set is a Cantor set, on which f_t is topologically conjugate to the shift $((\mathbb{Z}/2)^{\mathbb{N}}, \sigma)$.

It is easy to construct an expanding Markov partition for f_t, and therefore $\mathrm{H.\,dim}\, J(f_t)$ can be computed by the eigenvalue algorithm of §2. The results are plotted in Figure 10. The dotted line in the graph shows the asymptotic formula (6.1) below.

The family f_t, $t \in (0, 1]$ can be compared to the family of Schottky groups Γ_θ, $\theta \in (0, 2\pi/3]$ studied in §3, with a similar graph plotted in Figure 3. Both graphs display the variation of dimension as one moves from a highly expanding regime to a parabolic limit.

We will establish:

Theorem 6.1 *As $t \to 0$, we have*

$$\mathrm{H.\,dim}\, J(f_t) \sim \frac{\log 2}{\log\left(\frac{2}{t} - 1\right)} \asymp \frac{1}{|\log t|}, \tag{6.1}$$

while $\mathrm{H.\,dim}\, J(f_t) \to 1$ *as* $t \to 1$.

Proof. For t small the Julia set $J(f_t)$ is concentrated near the two repelling fixed-points $\{x_1, x_2\}$ of f_t, with $|x_i| \sim \sqrt{t}$. Let $\mathcal{P}$ be the Markov partition whose blocks $\{P_1, P_2\}$ are intervals of length t centered at $\{x_1, x_2\}$. We have $f(P_i) \supset P_1 \cup P_2$, and f_t is nearly linear on each block, so $\alpha(\mathcal{P})$ already provides a good approximation to δ, by the proof of Theorem 2.2. The highest eigenvalue of the transition matrix

$$T^\alpha_{ij} = \begin{pmatrix} u^\alpha & u^\alpha \\ u^\alpha & u^\alpha \end{pmatrix}$$

for $\mathcal{P}$ is simply $2u^\alpha$. Setting $u = |f'(x_i)| = 2/t - 1$, and solving for $\lambda(T^\alpha) = 1$, we obtain (6.1).

Since $J(f_t) = \widehat{\mathbb{R}}$, the behavior of the dimension as $t \to 1$ is a consequence of the continuity remarked upon above. ∎

Example II . For $r > 0$ let
$$f_r(z) = z + 1 - \frac{r}{z} \cdot$$
This map has a parabolic fixed-point with one petal at $z = \infty$, attracting both critical points of f_r. Thus we have $1/2 < \mathrm{H.dim}\, J(f_r) < 1$, and the dimension is a continuous function of r by [18, Thm 1.4]. We will establish:

Theorem 6.2 *For r small,*
$$\mathrm{H.dim}\, J(f_r) = \frac{1+\sqrt{r}}{2} + O(r),$$
while $\mathrm{H.dim}\, J(f_r) \to 1$ *as* $r \to \infty$.

Remark. The map $f_r(z)$ behaves like a coupling of the two generators of the Hecke group
$$H_r = \langle z \mapsto z+1, z \mapsto -r/z \rangle$$
considered (in a slightly different form) in §3, and we have
$$\mathrm{H.dim}(\Lambda(H_r)) = \frac{1}{2} + \sqrt{r} + O(r)$$
by Theorem 3.6. The estimates for $\mathrm{H.dim}\, J(f_r)$ and $\mathrm{H.dim}(\Lambda(H_r))$ follow the same line of argument. The difference between the coefficients of $\sqrt{r}$ in the two formulas comes from the fact that $\Lambda(H_r)$ clusters near $\mathbb{Z}$, while $J(f_r)$ clusters only near the integers $n \le 0$.

Proof of Theorem 6.2. Let μ be the canonical measure for f_r in the Euclidean metric, with dimension $\delta = \mathrm{H.dim}\, J(f_r)$.

For r small, the points $x > 2r$ are attracted to infinity; since f_r acts like a translation away from $x = 0$, $J(f_r)$ set is a Cantor set consisting of ∞ and pieces J_n concentrated near
$$x_n = f^{-n}(0) = -n(1 + O(r)),$$
$n \ge 0$. Since
$$\prod_1^\infty |f'(x_n)| = \prod (1 + r/x_n^2) = \prod (1 + O(r/n^2)) = 1 + O(r),$$
we have $|(f^n)'(x)|^\delta = 1 + O(r)$ on J_n, and thus
$$\mu(J_0) = \int_{J_n} |(f^n)'(x)|^\delta \, d\mu = \mu(J_n)(1 + O(r)).$$

Letting $g = f^{-1}$ denote the inverse branch of f with $g(J_n) \subset J_0$, we have $J_0 = \{0\} \cup \bigcup_1^\infty g(J_n)$, and $|g'(x)| = (r + O(r^2))/(n+1)^2$ on J_n. Therefore

$$\mu(J_0) \;=\; \sum_1^\infty \int_{J_n} |g'(x)|^\delta \, d\mu \;=\; \mu(J_0)(r^\delta + O(r^{1+\delta})) \sum (n+1)^{2\delta}.$$

From this equation we conclude $r^{-\delta} = \zeta(2\delta) + O(1)$, and since $\zeta(s) = (s-1)^{-1} + O(1)$ near $s = 0$, the desired estimate follows.

To treat the case $r \to \infty$, let $g_s = z + s - 1/z$ and note that $J(g_0) = \widehat{\mathbb{R}}$ as in Example I. It follows that

$$\lim_{s \to 0} \mathrm{H.dim}\, J(g_s) = \mathrm{H.dim}\, J(g_0) = 1.$$

Indeed, we have $J(g_s) \subset \widehat{\mathbb{R}}$ so $\limsup \mathrm{H.dim}\, J(g_s) \le 1$, and $\liminf \mathrm{H.dim}\, J(g_s) \ge \mathrm{H.dim}\, J(g_0) = 1$ by [18, Prop. 10.3]. Since $g_s(z)$ is conjugate to f_{1/s^2}, we find $\mathrm{H.dim}\, J(f_r) \to 1$ as well, as $r \to +\infty$. ∎

Remark. It would be interesting to find asymptotic formulas for the case of Blaschke products with $\mathrm{H.dim}\, J(f)$ near 1, akin to Theorems 3.5 and 3.6. One approach would be to relate the dimension of $J(f)$ to the least eigenvalue of the Laplacian on the Riemann surface lamination associated to f. (This lamination is discussed in [26]; see also [14].)

A Appendix: Dimension data

Markov partitions. Table 11 shows, for certain individual calculations, the size of the Markov partition $|\mathcal{P}|$ used to determine δ. These partitions were constructed by adaptive refinement of a given partition until $\max \operatorname{diam} P_i < r$ was achieved; the value of r is in column 3. Often some blocks of the partition were much smaller than r, especially in the presence of parabolic dynamics.

Object	$\lvert\mathcal{P}\rvert$	$\max \operatorname{diam} P_i$	δ
Apollonian gasket	1,397,616	0.000500	1.305688
Douady's rabbit	7,200,122	0.000025	1.3934(4)
$J(z^2-1)$	5,145,488	0.000012	1.26835
$J(z^2+1/4)$	1,209,680	0.000012	1.0812

Table 11. Markov partitions.

Schottky groups. The numerical values used to produce the graph of $\operatorname{H.dim} \Lambda_\theta$ in Figure 3 are presented in Table 12. The Markov partitions were refined to achieve $\max \operatorname{diam} P_i < 10^{-6}$, and $|\mathcal{P}|$ ranged from 6 to 600,000.

Quadratic polynomials. The values used for the graph of $\operatorname{H.dim} J(f_c)$ in Figure 8 are shown in Table 13. The Markov partitions were determined by $r = 10^{-4}$, and $|\mathcal{P}|$ varied in the range 50,000 to 500,000.

Blaschke products. The values used for the graph of $\operatorname{H.dim} J(f_t)$ in Figure 10 are shown in Table 13. The Markov partitions were determined by $r = 10^{-4}$, and $|\mathcal{P}|$ ranged from 4 to 30,000.

Angle	Dimension
1	0.06550651
2	0.07538293
3	0.08267478
4	0.08876751
5	0.09414988
6	0.09905804
7	0.10362620
8	0.10793886
9	0.11205308
10	0.11600945
11	0.11983805
12	0.12356187
13	0.12719898
14	0.13076388
15	0.13426843
16	0.13772248
17	0.14113438
18	0.14451124
19	0.14785921
20	0.15118368
21	0.15448941
22	0.15778064
23	0.16106117
24	0.16433446
25	0.16760366
26	0.17087168
27	0.17414119
28	0.17741472
29	0.18069460
30	0.18398306

Angle	Dimension
31	0.18728221
32	0.19059405
33	0.19392052
34	0.19726349
35	0.20062475
36	0.20400606
37	0.20740915
38	0.21083570
39	0.21428737
40	0.21776581
41	0.22127266
42	0.22480954
43	0.22837808
44	0.23197992
45	0.23561668
46	0.23929002
47	0.24300162
48	0.24675315
49	0.25054633
50	0.25438290
51	0.25826464
52	0.26219335
53	0.26617088
54	0.27019914
55	0.27428006
56	0.27841564
57	0.28260792
58	0.28685903
59	0.29117113
60	0.29554648

Angle	Dimension
61	0.29998740
62	0.30449628
63	0.30907563
64	0.31372802
65	0.31845614
66	0.32326275
67	0.32815077
68	0.33312320
69	0.33818318
70	0.34333400
71	0.34857906
72	0.35392195
73	0.35936641
74	0.36491635
75	0.37057588
76	0.37634931
77	0.38224116
78	0.38825619
79	0.39439942
80	0.40067613
81	0.40709188
82	0.41365257
83	0.42036442
84	0.42723402
85	0.43426838
86	0.44147493
87	0.44886156
88	0.45643671
89	0.46420936
90	0.47218913

Angle	Dimension
91	0.48038631
92	0.48881197
93	0.49747800
94	0.50639724
95	0.51558356
96	0.52505200
97	0.53481894
98	0.54490222
99	0.55532142
100	0.56609805
101	0.57725587
102	0.58882126
103	0.60082369
104	0.61329624
105	0.62627635
106	0.63980676
107	0.65393666
108	0.66872334
109	0.68423436
110	0.70055063
111	0.71777084
112	0.73601807
113	0.75545018
114	0.77627694
115	0.79879030
116	0.82342329
117	0.85087982
118	0.88248407
119	0.92152480
120	1.00000000

Table 12. Dimension data for 3-generator Schottky groups.

C	Dim
-1.000	1.2683
-0.990	1.2671
-0.980	1.2661
-0.970	1.2652
-0.960	1.2643
-0.950	1.2635
-0.940	1.2628
-0.930	1.2621
-0.920	1.2614
-0.910	1.2608
-0.900	1.2603
-0.890	1.2597
-0.880	1.2592
-0.870	1.2586
-0.860	1.2581
-0.850	1.2575
-0.840	1.2568
-0.830	1.2560
-0.820	1.2552
-0.810	1.2541
-0.800	1.2529
-0.790	1.2513
-0.780	1.2494
-0.770	1.2468
-0.760	1.2430
-0.750	1.2342
-0.740	1.2170
-0.730	1.2046
-0.720	1.1939
-0.710	1.1844

C	Dim
-0.700	1.1757
-0.690	1.1677
-0.680	1.1602
-0.670	1.1531
-0.660	1.1465
-0.650	1.1402
-0.640	1.1343
-0.630	1.1286
-0.620	1.1232
-0.610	1.1180
-0.600	1.1131
-0.590	1.1084
-0.580	1.1039
-0.570	1.0995
-0.560	1.0954
-0.550	1.0914
-0.540	1.0875
-0.530	1.0838
-0.520	1.0802
-0.510	1.0767
-0.500	1.0734
-0.490	1.0702
-0.480	1.0671
-0.470	1.0641
-0.460	1.0612
-0.450	1.0584
-0.440	1.0557
-0.430	1.0530
-0.420	1.0505
-0.410	1.0481

C	Dim
-0.400	1.0457
-0.390	1.0434
-0.380	1.0412
-0.370	1.0390
-0.360	1.0369
-0.350	1.0349
-0.340	1.0330
-0.330	1.0311
-0.320	1.0293
-0.310	1.0275
-0.300	1.0258
-0.290	1.0242
-0.280	1.0226
-0.270	1.0210
-0.260	1.0196
-0.250	1.0182
-0.240	1.0168
-0.230	1.0155
-0.220	1.0142
-0.210	1.0130
-0.200	1.0119
-0.190	1.0108
-0.180	1.0097
-0.170	1.0087
-0.160	1.0078
-0.150	1.0069
-0.140	1.0060
-0.130	1.0052
-0.120	1.0045
-0.110	1.0038

C	Dim
-0.100	1.0032
-0.090	1.0026
-0.080	1.0020
-0.070	1.0016
-0.060	1.0012
-0.050	1.0008
-0.040	1.0005
-0.030	1.0003
-0.020	1.0001
-0.010	1.0000
0.000	1.0000
0.010	1.0000
0.020	1.0001
0.030	1.0003
0.040	1.0006
0.050	1.0009
0.060	1.0014
0.070	1.0020
0.080	1.0026
0.090	1.0034
0.100	1.0043
0.110	1.0054
0.120	1.0066
0.130	1.0080
0.140	1.0096
0.150	1.0114
0.160	1.0135
0.170	1.0159
0.180	1.0187
0.190	1.0219

C	Dim
0.200	1.0257
0.210	1.0302
0.220	1.0358
0.230	1.0431
0.240	1.0537
0.250	1.0812
0.260	1.3355
0.270	1.3093
0.280	1.2879
0.290	1.2690
0.300	1.2518
0.310	1.2357
0.320	1.2206
0.330	1.2063
0.340	1.1927
0.350	1.1796
0.360	1.1671
0.370	1.1551
0.380	1.1435
0.390	1.1324
0.400	1.1216
0.410	1.1111
0.420	1.1010
0.430	1.0912
0.440	1.0817
0.450	1.0724
0.460	1.0635
0.470	1.0547
0.480	1.0462
0.490	1.0380
0.500	1.0299

Table 13. Dimension data for the Julia set of $z^2 + c$.

t	Dimension
0.01	0.13082375
0.02	0.15051361
0.03	0.16504294
0.04	0.17717636
0.05	0.18788888
0.06	0.19765129
0.07	0.20673100
0.08	0.21529616
0.09	0.22346020
0.10	0.23130367
0.11	0.23888612
0.12	0.24625297
0.13	0.25343977
0.14	0.26047497
0.15	0.26738172
0.16	0.27417918
0.17	0.28088343
0.18	0.28750812
0.19	0.29406496
0.20	0.30056411
0.21	0.30701444
0.22	0.31342379
0.23	0.31979909
0.24	0.32614657
0.25	0.33247183
0.26	0.33877992
0.27	0.34507545
0.28	0.35136268
0.29	0.35764548
0.30	0.36392743
0.31	0.37021191
0.32	0.37650202
0.33	0.38280070
0.34	0.38911070
0.35	0.39543465
0.36	0.40177499
0.37	0.40813411
0.38	0.41451429
0.39	0.42091770
0.40	0.42734640
0.41	0.43380242
0.42	0.44028773
0.43	0.44680428
0.44	0.45335394
0.45	0.45993849
0.46	0.46655981
0.47	0.47321969
0.48	0.47991987
0.49	0.48666212
0.50	0.49344815
0.51	0.50027971
0.52	0.50715853
0.53	0.51408651
0.54	0.52106538
0.55	0.52809698
0.56	0.53518305
0.57	0.54232547
0.58	0.54952609
0.59	0.55678688
0.60	0.56410985
0.61	0.57149710
0.62	0.57895073
0.63	0.58647284
0.64	0.59406594
0.65	0.60173223
0.66	0.60947418
0.67	0.61729440
0.68	0.62519554
0.69	0.63318064
0.70	0.64125285
0.71	0.64941525
0.72	0.65767136
0.73	0.66602497
0.74	0.67448006
0.75	0.68304083
0.76	0.69171216
0.77	0.70049926
0.78	0.70940743
0.79	0.71844298
0.80	0.72761282
0.81	0.73692474
0.82	0.74638718
0.83	0.75601000
0.84	0.76580402
0.85	0.77578241
0.86	0.78595974
0.87	0.79635345
0.88	0.80698440
0.89	0.81787755
0.90	0.82906362
0.91	0.84058100
0.92	0.85247928
0.93	0.86482346
0.94	0.87770228
0.95	0.89124297
0.96	0.90564092
0.97	0.92122117
0.98	0.93861440
0.99	0.95942792
1.00	1.00000000

Table 14. Dimension data for the Julia set of $z/t + 1/z$.

References

[1] J. Anderson and A. Rocha. Analyticity of Hausdorff dimension of limit sets of Kleinian groups. *Ann. Acad. Sci. Fenn.* **22**(1997), 349–364.

[2] A. Beardon. The exponent of convergence of the Poincaré series. *Proc. London Math. Soc.* **18**(1968), 461–483.

[3] O. Bodart and M. Zinsmeister. Quelques résultats sur la dimension de Hausdorff des ensembles de Julia des polynômes quadratiques. *Fund. Math.* **151**(1996), 121–137.

[4] R. Bowen. Hausdorff dimension of quasi-circles. *IHES Publ. Math.* **50**(1978), 11–25.

[5] D. Boyd. The residual set dimension of the Apollonian packing. *Mathematika* **20**(1973), 170–174.

[6] L. Carleson and T. Gamelin. *Complex Dynamics*. Springer-Verlag, 1993.

[7] J. Dodziuk, T. Pignataro, B. Randol, and D. Sullivan. Estimating small eigenvalues of Riemann surfaces. In *The Legacy of Sonya Kovalevskaya*, Contemp. Math., 64, pages 93–121. Amer. Math. Soc, 1987.

[8] A. Douady and J. Hubbard. *Étude dynamique des polynômes complexes*. Pub. Math. d'Orsay 84–2, 85–4, 1985.

[9] A. Douady, P. Sentenac, and M. Zinsmeister. Implosion parabolique et dimension de Hausdorff. *C. R. Acad. Sci. Paris Sér. I Math.* **325**(1997), 765–772.

[10] P. Doyle. On the bass note of a Schottky group. *Acta Math.* **160**(1988), 249–284.

[11] K. J. Falconer. *The Geometry of Fractal Sets*. Cambridge University Press, 1986.

[12] F. R. Gantmacher. *The Theory of Matrices*, volume II. Chelsea, 1959.

[13] R. J. Gardner and R. D. Mauldin. On the Hausdorff dimension of a set of complex continued fractions. *Illinois J. Math.* **27**(1983), 334–345.

[14] M. Lyubich and Y. Minsky. Laminations in holomorphic dynamics. *J. Diff. Geom.* **47**(1997), 17–94.

[15] P. Mattila. *Geometry of Sets and Measures in Euclidean Spaces.* Cambridge University Press, 1995.

[16] C. McMullen. *Complex Dynamics and Renormalization*, volume 135 of *Annals of Math. Studies.* Princeton University Press, 1994.

[17] C. McMullen. Hausdorff dimension and conformal dynamics I: Kleinian groups and strong limits. *J. Diff. Geom.* **51**(1999), 471–515.

[18] C. McMullen. Hausdorff dimension and conformal dynamics II: Geometrically finite rational maps. *Comm. Math. Helv.* **75**(2000), 535–593.

[19] C. McMullen. Calculating the exponent of divergence of the Poincaré series. *Preprint, Harvard, 1984.*

[20] J. Milnor. *Dynamics in One Complex Variable: Introductory Lectures.* Vieweg, 1999.

[21] R. Phillips and P. Sarnak. The Laplacian for domains in hyperbolic space and limit sets of Kleinian groups. *Acta Math.* **155**(1985), 173–241.

[22] D. Ruelle. Repellers for real analytic maps. *Ergod. Th. & Dynam. Sys.* **2**(1982), 99–107.

[23] R. S. Strichartz, A. Taylor, and T. Zhang. Densities of self-similar measures on the line. *Experiment. Math.* **4**(1995), 101–128.

[24] D. Sullivan. Entropy, Hausdorff measures new and old and limit sets of geometrically finite Kleinian groups. *Acta Math.* **153**(1984), 259–277.

[25] D. Sullivan. Related aspects of positivity in Riemannian geometry. *J. Diff. Geom.* **25**(1987), 327–351.

[26] D. Sullivan. Linking the universalities of Milnor-Thurston, Feigenbaum and Ahlfors-Bers. In L. R. Goldberg and A. V. Phillips, editors, *Topological Methods in Modern Mathematics*, pages 543–564. Publish or Perish, Inc., 1993.

[27] Tan L. and Yin Y. Local connectivity of the Julia set for geometrically finite rational maps. *Science in China (Series A)* **39**(1996), 39–47.

[28] M. Widom, D. Bensimon, and L. Kadanoff. Strange objects in the complex plane. *J. Statist. Phys.* **32**(1983), 443–454.

[29] M. Zinsmeister. *Formalisme thermodynamique et systèmes dynamiques holomorphes.* Société Mathématique de France, 1996.

Mathematics Department, Harvard University, 1 Oxford St, Cambridge, MA 02138-2901